Bedrock deformations in northeastern Estonia based on ground-penetrating radar data

Argo Jõeleht[a*], Ivo Sibul[a,b], Mario Mustasaar[a] and Jüri Plado[a]

[a] Department of Geology, University of Tartu, Ravila 14A, 50411 Tartu, Estonia; mustasaarmario@gmail.com, juri.plado@ut.ee
[b] Department of Geology, Estonian Land Board, Mustamäe tee 51, 10621 Tallinn, Estonia; ivo.sibul@maaamet.ee

*Corresponding author, argo.joeleht@ut.ee

Received 5 July 2022, accepted 6 November 2022, available online 27 November 2022

Abstract. The Vaivara Deformation Zone (VDZ) in northeastern Estonia was studied with ground-penetrating radar (GPR). While the typical Paleozoic carbonate plateau in northern Estonia is characterized by a subhorizontal continuous reflection pattern in GPR images, the VDZ, located south of the erosional bedrock escarpment, known as the Baltic Klint, frequently contains deformed and tilted limestone blocks, thrusts, and folds. We categorize the structural features seen in the GPR images according to deformation intensity and show their areal distribution. In addition to the VDZ, bedrock segments are deformed in Tõrvajõe village, the Pähklimäed Hills, and Narva town, whereas the distribution and nature of deformations hint at a glaciotectonic origin. The study confirms that GPR is a suitable tool for discovering and interpreting bedrock structures. Auxiliary geological and geophysical techniques are required for outlining of bedrock blocks.

Keywords: Glaciotectonic deformations, Paleozoic bedrock, Quaternary, ground-penetrating radar, Vaivara Deformation Zone, Sinimäed, Narva, Estonia.

INTRODUCTION

Quaternary glaciotectonic structures have been identified in formerly ice-covered regions in Europe and northern America (Aber and Ber 2007), as well as in Iceland, Antarctica, and other areas where glaciers are currently present (Ingólfsson et al. 2016; Fitzsimons and Howarth 2020). Ground-penetrating radar (GPR) has been widely applied for describing the general layout and inner morphology of these structures. Generally, deformations are associated with tills (Møller and Jakobsen 2002; Bakker and van der Meer 2003), glaciofluvial sediments (Overgaard and Jakobsen 2001; Pasanen 2009) or other types of unconsolidated strata (Busby and Merritt 1999; Brandes and Le Heron 2010). However, so far, the results of glaciotectonic movements within the brittle sedimentary rocks have not been described in detail.

Northern Estonia is generally characterized by a smooth, undisturbed limestone plateau, covered by a thin sequence of Quaternary sediments and bounded by a cliff, the Baltic Klint, along the southern coast of the Gulf of Finland. The plateau is occasionally articulated by positive landforms, which are up to 40–50 m higher than the surrounding areas (Karukäpp and Raukas 1997). For example, in northeastern Estonia, between Sillamäe and Narva towns, the 3 km long and 0.3 km wide hill ridge of Sinimäed emerges from the otherwise flat terrain, representing unusual positive landforms in the area (Fig. 1).

The Baltic Klint in the north, the Sinimäed Hills and positive landforms near Laagna village in the south, and the Narva River lowland in the east border an area about 13 km long and 2 to 3 km wide (Fig. 1) that includes numerous bedrock displacements. Suuroja and Ploom (2016) named the western part of the area the Vaivara Dislocation Zone. We prefer to use the term "Vaivara Deformation Zone" (VDZ) as besides horizontal and vertical movements, the region also consists of *in situ* deformations of different intensities.

The origin of the VDZ, especially of the three Sinimäed Hills, has been widely discussed: Volin (1974) and Lobanov (1976) noticed their similarities with Duderhof Heights in the southwestern part of St. Petersburg (Russia) and suggested diapirism as the forming mechanism for both. Raukas (1995), later Rattas and Kalm (2004), inter-

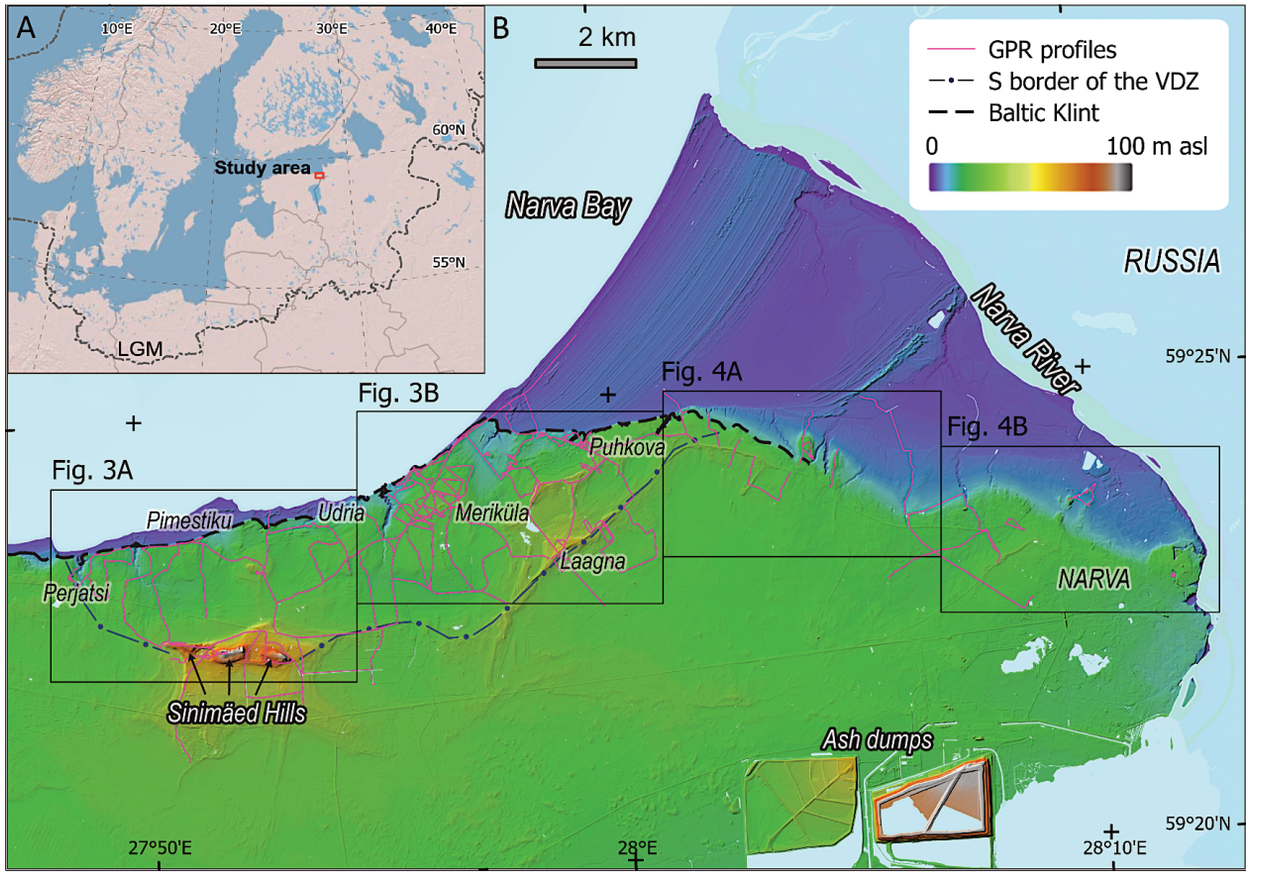

Fig. 1. A – Overview map (shaded relief image) showing the location of the study area. LGM represents the Last Glacial Maximum (after Ehlers and Gibbard 2003). B – Ground-penetrating radar (GPR) profiles carried out in the region. The study area is bordered by the Baltic Klint in the north (these data, along with LiDAR elevation data, are from the Estonian Land Board) and by the border of the Vaivara Deformation Zone (VDZ) in the south (current interpretation).

preted the Sinimäed Hills as limestone blocks torn apart from the Baltic Klint and transported some kilometers southwards by glaciers. Alternative hypotheses by Puura and Vaher (1997) propose that the ridge has been formed either by a continental ice sheet (terminal moraine), clay diapirism, or their combination. The most recent geological mapping campaign (Suuroja et al. 2009a, 2009b) led to the opinion that the hills were assembled by a series of glaciations which crushed the limestone plateau; thus, later glaciations could fold and erode the disrupted bedrock blocks more easily. Suuroja and Ploom (2016) favored the diapiric origin of the hills, with the addition that the Cambrian blue clay flow in fault zones was induced by a load of continental glaciers. Vaher et al. (2013) concluded that the diapiric origin of the easternmost hill in the ridge might also extend to the other two hills.

The aim of this study was to locate and characterize deformations within the VDZ by using GPR. To provide a broader picture of the glaciotectonic activities, the initial study area (VDZ) was extended eastwards to Narva town. We highlight that GPR can only visualize the topmost subsurface. Other geological or geophysical methods, such as seismic, electric, or electromagnetic, should be applied to more in-depth studies. At the same time, GPR is a fast method for locating areas of interest; thus, it is a primary tool for field geologists/geophysicists. The explicit origin of deformations is beyond the scope of the present paper. Nevertheless, some aspects concerning the complexity and possible forming mechanisms of the deformations will be discussed below.

GEOLOGICAL SETTING

The study area (Fig. 1), extending a few kilometers south of the Baltic Klint, is located on the southern slope of the Fennoscandian Shield, where the Quaternary succession, underlain by Ordovician, Cambrian, and Ediacaran car-

bonate and terrigenous sediments, cover the Paleo proterozoic Svecofennian crystalline basement. Quaternary overburden is missing in the immediate vicinity of the Klint. In the accumulative landforms, however, the thickness of the Quaternary reaches 15 m (Suuroja et al. 2009a, 2009b). The dominating sediment types are gravel, sand, and glacial till.

Ordovician sedimentary rocks with a total thickness of up to about 20 m constitute the topmost part of the bedrock. The Ordovician succession is mainly composed of limestones and dolostones, whereas its basal part is represented by sandstones, argillites, and clays, overlain by glauconitic sand- and siltstones. In undeformed positions, the thickness of Ordovician rocks increases gently from north to south, following the typical decline (8–15' or 2–4 m/km) of the whole sedimentary bedrock (Meidla 2014; Tuuling and Flodén 2016).

Cambrian clay, siltstone, and sandstone underlying the Ordovician sediments are exposed under Quaternary sediments north of the Baltic Klint and in the basal parts of the buried valleys incising south from the cliff. The lower part of the Cambrian (late Terreneuvian and early Series 2) is composed of a 75–120 m thick silty clay unit, also known by the term "blue clay", which is plastic despite its age (529–514 Ma). While the top of the blue clay unit is expected to occur a few meters above sea level near the coastline at the study area, the drilling data frequently indicate clay outcropping on the ground surface (about 30–40 m above the average level) between Perjatsi and Meriküla villages (Suuroja et al. 2009a, 2009b). This region forms the main part of the WSW-ENE-oriented belt of bedrock deformations, the VDZ, which is about 13 km long (Fig. 1). In this zone, a borehole north of the Sinimäed Hills (#314, see Fig. 3A) reveals 120 m of Cambrian blue clay deposits that are ~40 m thicker than normal. The upper part of the drill core shows many deformational features (e.g., tilting of strata up to 90°, faults, slickensides and repeated stratigraphy), the quantity of which decreases with depth. The basal part of the blue clay and underlying Ediacaran (mainly sandstone-silty clay-sandstone complex with a total thickness of 120 m) is not deformed and has the expected thicknesses/depths (Suuroja et al. 2009b).

METHODS

Ground-penetrating radar fieldworks were conducted with the Zond-12e system by Radar Systems Inc. Low-frequency (100 and 300 MHz) common offset antennas were used on roads where the antennas were towed by a car. Meadows and sites with natural obstacles (shrub and ditches) were investigated with 300 MHz common-offset antennas pulled by the researchers. An odometer wheel measured the distances and triggered GPR signals at a constant spacing of 0.1 m. The measurements were coordinated with a portable GPS instrument (Altina GGM309; estimated positional accuracy 3–5 m in an open field, up to 15 m in the forest) connected to a radar device. To amplify reflections and reduce the noise level, stacking of 2 or 4 measurements was applied. Altogether, 170 km of profiles were run.

Data processing with the Prism2 software included a bandpass filter for removing occasional low-frequency interference. A time-dependent gain was applied to amplify the deepest reflections. Background removal was not needed as geological patterns/surfaces can be discriminated from flat instrumental noise. Topographic corrections were based on the Estonian Land Board's LiDAR data and were applied to the profile every 10 m. To convert the two-way travel time to depth scale, the electromagnetic wave velocity (V_{EMW}) was determined by utilizing the hyperbola fitting technique (Shihab et al. 2004). The determination was carried out at several locations, characterizing different geological conditions. The obtained values varied from 8.7 cm ns^{-1} to 10.0 cm ns^{-1}, whereas the average (9.3 cm n^{-1}) was used for all the profiles. The obtained speed is comparable to values that have been measured in similar conditions (Jõeleht and Plado 2010; Mustasaar et al. 2011; Sibul et al. 2017). The signal penetration was typically between 2 and 4 m. The radar images were interpreted visually by tracing the profile segments with identifiable reflections. The segments were classified, described, grouped, and mapped.

RESULTS

Reflectivity and lithological patterns

The geological composition in the radar images was designated based on the reflection patterns and relative amplitude of the electromagnetic signal. The typical reflection pattern of Middle Ordovician limestone in northern Estonia consists of densely spaced continuous reflectors with few hyperbolic reflections from layer-parallel caverns or fractures. Reflections in radargrams exhibit low (up to few decimeters) short-wavelength undulations due to microtopography, which cannot be appropriately included in topographic corrections.

Hence, the most widespread and uniquely identifiable are the sedimentary carbonate layers under thin (< 1 m) overburden (Fig. 2A). The carbonate rocks have a characteristic pattern of irregularly spaced reflections that can be continuously followed laterally over a long distance. However, the lowermost part of the carbonate rock sequence, the Toila Formation (late Floian–Dapingian in age), is rich in clay, and thus attenuates electromagnetic

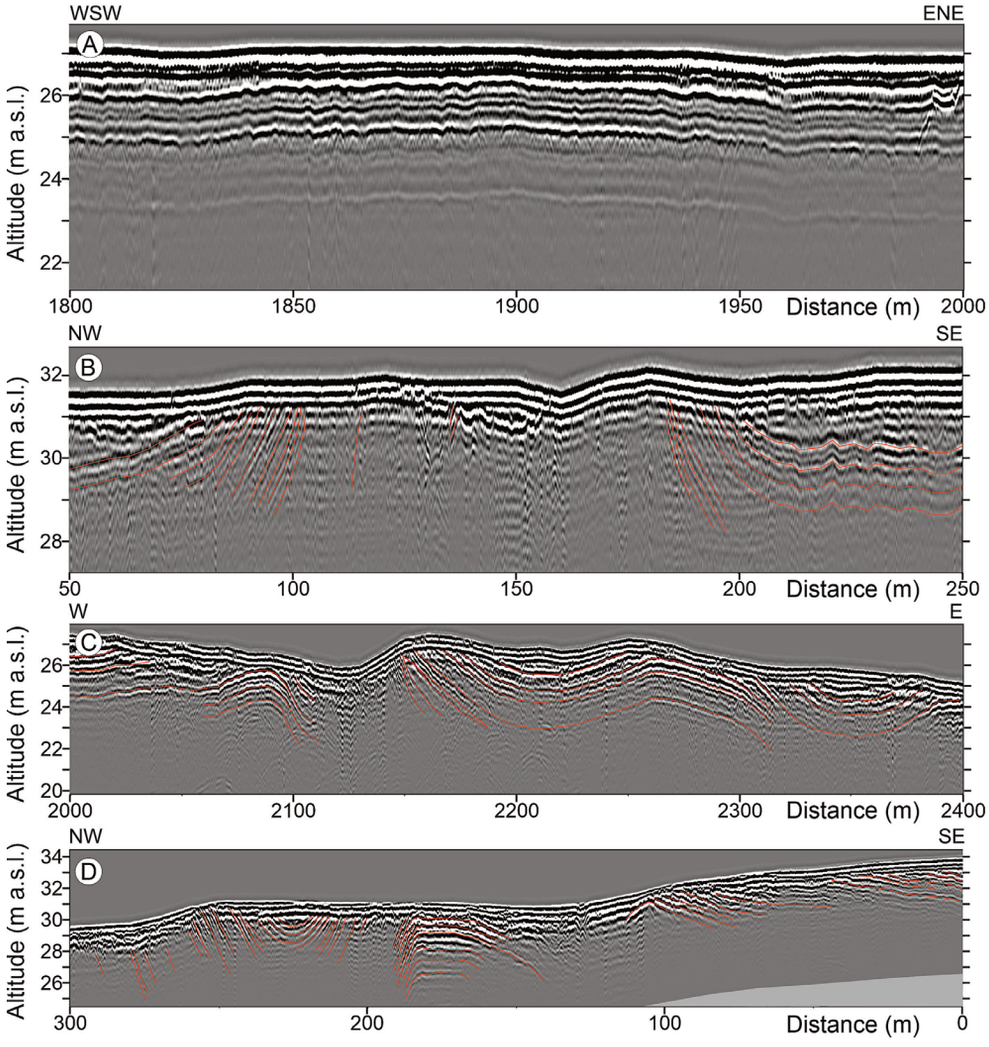

Fig. 2. Examples of radar images with different degrees of deformation. A – In non-deformed areas, reflections in carbonate rocks are subhorizontal or follow regional tilting in the SSE direction. B – Anticlinal structure between weakly deformed limestone blocks. Note the lack of fold-related topographic features. C – Two limestone blocks (at distances of 2000–2120 m and 2140–2400 m) with wavy bedding. Typically for that kind of deformed blocks, their margins can be turned upward and downward. D – Large uniformly tilted Sõmerkallas block (at a distance of 0–100 m) in the SE is bounded in the NW by a zone of folds and thrusts that have a ridge-like appearance on the Digital Elevation Model (DEM). Red lines mark layering-related reflectors. The sections have a vertical exaggeration of ~10x. See Figs 3 and 4 for the location of the images.

signals well. Increased attenuation is a characteristic and sometimes helpful feature that can be used to recognize lithostratigraphic units.

The Lower Ordovician and Cambrian sandstones outcrop mainly in topographic lows where the limestone cover is missing, and in the axial part of anticlines. Occasionally, sandstone and limestone may have similar reflection patterns. Nevertheless, at a closer look, the reflections originating from sandstone are of more variable amplitude, laterally less continuous reflectors that instead tend to merge or wedge out. The not so well-developed layered structure of sandstone in the radar images is caused by cross-bedding of the target sandstone formation.

Deformations and their intensity

Radar images show flat-lying bedrock and reveal considerable deformations in the VDZ, ranging from slightly tilted or wavy limestone to intense folding and even tilted blocks with a ribbed appearance. In undisturbed areas, the reflectors follow a regional gentle (7–9' or 2.0–2.5 m/km)

dip of the Estonian Homocline in the southern or southeastern direction. In the less disturbed areas of the VDZ, the apparent dip along the profiles varies from a few degrees in the central part of the larger limestone blocks (1–2 km long and hundreds of m wide) to more than 10° in the block margins (Fig. 2B). Larger blocks that are often elongated in the SW–NE direction have a tilt towards SE. Smaller blocks that seem to be non-elongated have wavy bedding with a variable dip direction. Radar images indicate subhorizontal bedding that typically maintains modest reflector altitude variations (up to 2 meters) over 50–100 m distances (Fig. 2C). The margins of both the monoclinally tilted larger blocks and the wavy-bedded smaller blocks are usually steeper, with a dip generally less than 10°, but occasionally reaching at least 40°. The block margins can be tilted either upward or downward (e.g., Fig. 2C), but in general, the margins of large blocks seem to be more often turned upward (e.g., Fig. 2B).

In many locations, radar sections showed strongly folded limestone (Fig. 2D) and imbricated thrusting. Such deformation structures can be visually observed in nature as 1–2 m high narrow ridges that sometimes occur as a single ridge, but more often as a set of ridges with a spacing of 60–100 m between the ridge axes. These linear ridges are also identifiable on the shaded relief image (Fig. 3, e.g., between the Baltic Klint and Sõmerkallas), suggesting that the ridges vary in length from a few hundred meters to 1.5 km. The core of the ridges is usually formed of variably tilted limestone. Visual inspection revealed limestone blocks with a dip angle of up to 90°, but such steep dipping is not identifiable by radar. The apparent dip angle of the blocks detected by GPR varied from 4 to 40°.

DISCUSSION

Classification of deformation types

The GPR data combined with the Digital Elevation Model (DEM) allow us to distinguish geological features and their distribution (Figs 3 and 4). Based on the reflection patterns in the GPR images, the bedrock deformation features were divided into several categories. These types are linked to ancient horizontal stress conditions and lateral shortening of strata in ascending order.

Type I deformations usually occur within the carbonate bedrock block. In the GPR images, type I deformations are represented by subhorizontal wavy bedding with vertical undulation of the reflections up to 2–3 m per 100 m in the horizontal direction. The reflections continue for at least a few hundred meters and sometimes resemble normal (undeformed) bedding. However, measurements, especially those acquired perpendicular to the strike, reveal bending and/or tilting of the strata, which exceeds the regional dip. Compared to the following types, the deformations are due to low horizontal stress conditions and little lateral shortening.

Two varieties of type I occur, based on the wavelengths of folding. Subtype I^a with a shorter wavelength (fold-to-fold distance from tens of meters to a couple of hundred meters) is represented by thin (thickness up to 10 m) carbonate bedrock blocks that have been distributed over irregularly undulating basal topography. Subtype I^b with a longer wavelength is internally less disturbed, tilt angles change smoothly over the distance from one hundred meters to several hundred meters. This suggests thicker blocks that are not only limited to carbonate rocks. However, these blocks have been moved away from their sedimentary positions as indicated by deformations at their boundaries (Fig. 2B).

Type II deformations with inclined bedding (with apparent tilting of >3 m per 100 m; Fig. 2C) are observed at the margins of large carbonate rock blocks but can also form zones of folded bedrock. Due to the steeper dip compared to type I, it can be difficult to track bedrock reflectors and, thus, confirm the continuation of bedrock blocks over several tens of meters. Here and there, it is rather obscure whether bedrock bedding has been disrupted due to faults within one block, or whether separate blocks exist.

Type III includes bedrock deformations represented by thrusting and extensive folding (Fig. 2D). In contrast to type II, type III deformations are visible in the topography in the form of elongated ridges. The ridges are typically NE–SW oriented, parallel to each other, and occur 1–2 km south of the Klint (Fig. 3), except between Udria and Meriküla villages. While type II marks the marginal zone of the bedrock blocks and thus the deformation zones are of different orientations, type III seems to be related to intensive horizontal stress condition and high lateral shortening.

Areal distribution of deformations

The GPR data provides an insight into the underlying strata, revealing hectic arrangement of deformation structures and abrupt changes in the geological setting within a few tens of meters. However, clayey soil, road fill, thick vegetation, and other local conditions may hinder the visibility of GPR images. Other data sources such as the DEM, orthophoto, and drain network were used for distinguishing geological features and their distribution within the study area (Figs 3 and 4). Despite the efforts, these data alone were not sufficient to outline the carbonate bedrock blocks over the VDZ. Some characteristic and prominent locations are discussed in detail below.

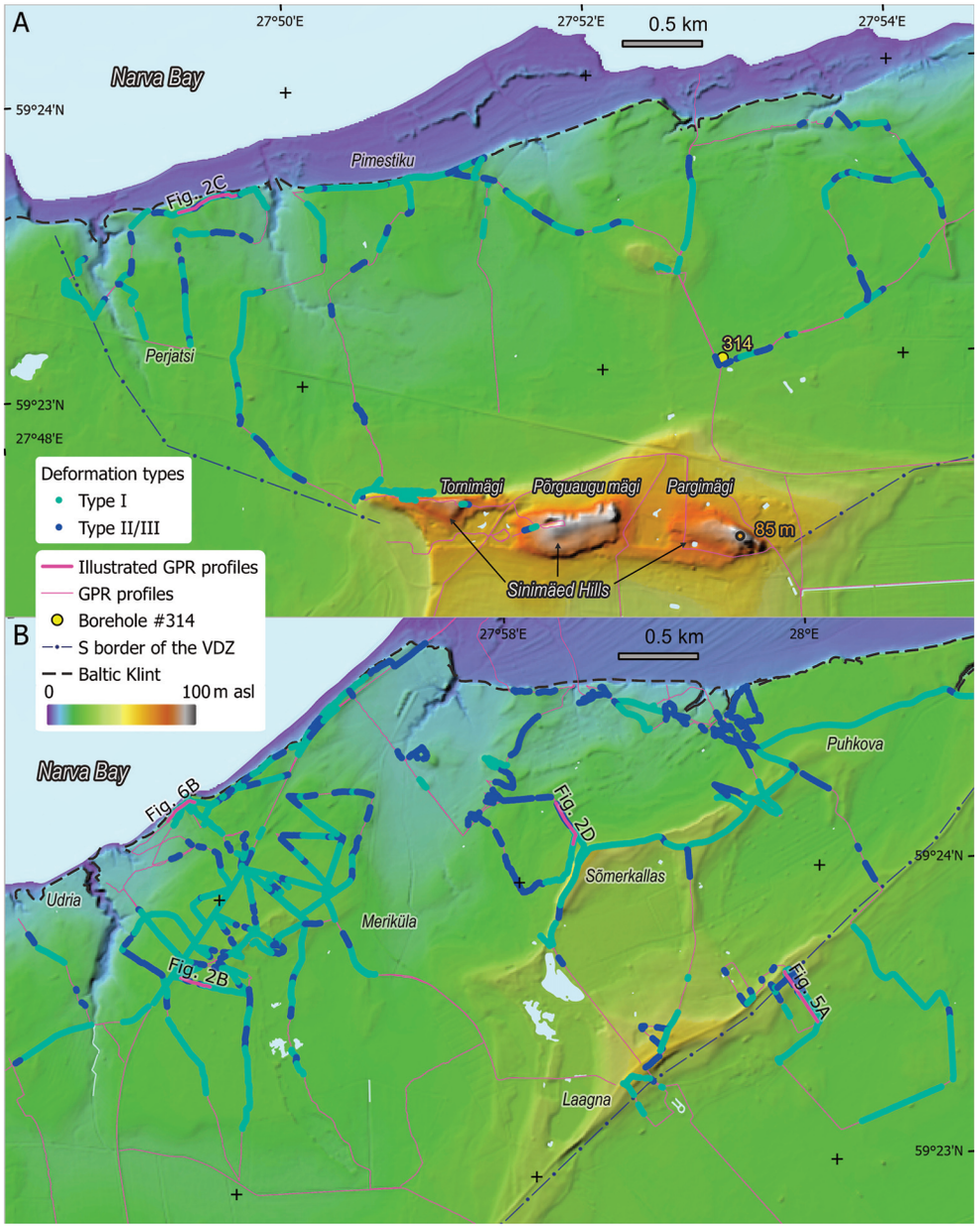

Fig. 3. Bedrock structures according to GPR within the study areas (A) and (B) (for locations, see Fig. 1) on top of the shaded relief image. Reflections in the GPR images were classified by deformation intensity (types I–III are described in the text).

Sinimäed Hills and Laagna heights

The Sinimäed Hills (Fig. 3A) are composed of three individual hillocks named Tornimägi (Tower Hill), Põrguaugu mägi (Hill of Hell's Hole), and Pargimägi (Park Hill). Two NE–SW oriented elongated heights are located near Laagna village (Fig. 3B). The northern section of the Laagna heights, also known as the erratic bank of Sõmerkallas (Suuroja et al. 2009a), resembles Tornimägi. Both Tornimägi and Sõmerkallas have a core of sizeable limestone-topped megablock elevated relative to the surrounding area. The core block is densely fractured, yet otherwise intact, having strong deformations only at the lateral ends. The core block of Tornimägi is 150 m wide and at least 700 m long. The northeastern part of the bank of Sõmerkallas lowers gradually and continues as another block, which is 300–400 m wide, but more than 2 km long. Both Tornimägi and the hills of Sõmerkallas have a cliff in the northern/northeastern face, whereas the relatively monolithic core is tilted in southern/

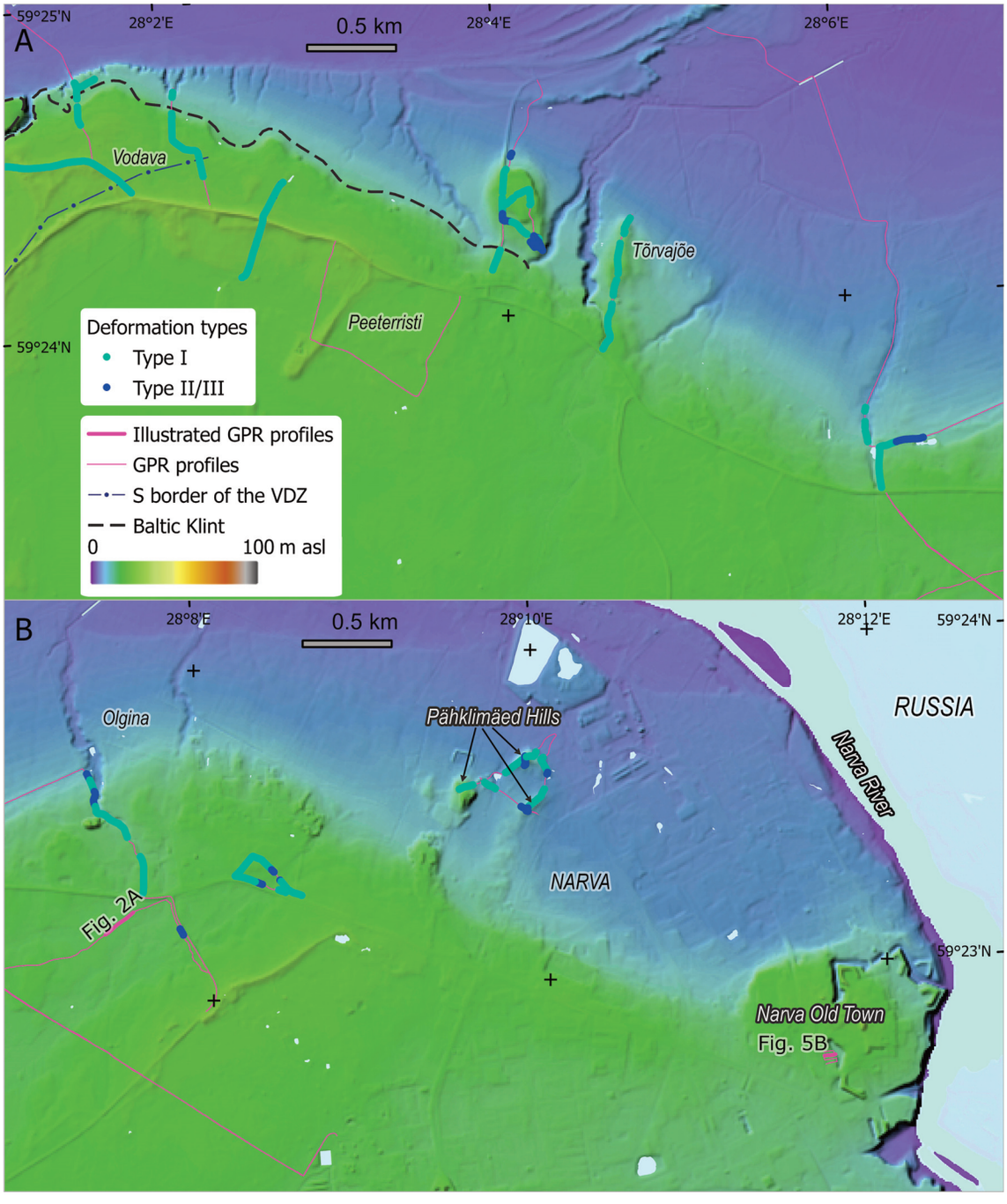

Fig. 4. Bedrock structures according to GPR within the study areas (A) and (B) (for locations, see Fig. 1) on top of the shaded relief image. Reflections in the GPR images were classified by deformation intensity (types I–III are described in the text).

southeastern directions at an angle of 10° and 5°, respectively.

The southern one of the Laagna heights, also known as the Laagna rise, has a completely different internal structure than the bank of Sõmerkallas, as there does not appear to be a monolithic core. Instead, the rise consists of limestone and sandstone blocks that are uplifted up to 15 m above the surrounding terrain, folded and tilted (Fig. 5A). The size of the blocks is at least several tens of meters.

There is no clear arrangement in the direction of tilting. The apparent dip angle of the uplifted blocks varies from 7 to 25°, with a tendency of steeper tilting at block

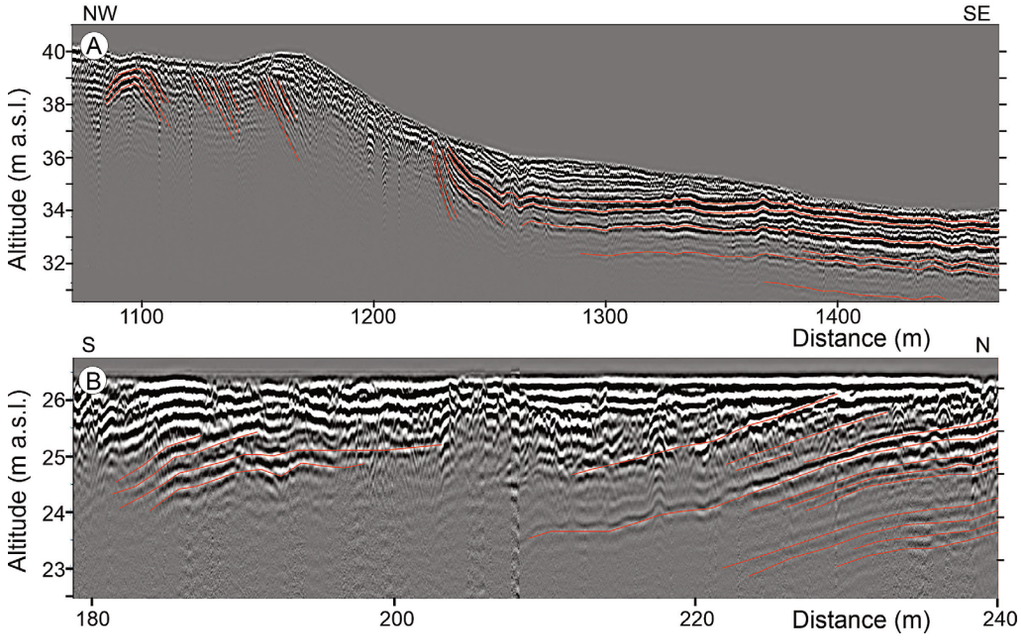

Fig. 5. A – Radar image shows the blocky internal structure of the Laagna rise in the NW part of the section and the transition to weakly deformed bedrock towards the SE of the VDZ. B – Radar image of the Narva block. The reflections that originate from carbonate rock layers dip westward at 3.2° and are, thus, in contrast to a modest regional tilt in the SSE direction. The vertical exaggeration equals to ~2.4x.

margins. The margins of individual limestone blocks can show over-thrusting or upward bending of the limestones, with the anticline core being formed of material that has no internal reflectivity, such as sand, (blue?) clay, or till. One of the pronounced anticlinal structures was found at the southeastern foothill of the Laagna rise.

Udria cliff and plateau

At first glance, the Udria cliff is a typical section of the Baltic Klint (Fig. 6A). The GPR profile near the cliff edge shows wavy bedding of carbonate rocks that thin out westwards (Fig. 6B). At a closer look, the outcrop also reveals an increase in deformations in the westward direction. Intercalated sand and argillite of the Lower Ordovician in the east (Fig. 6C) is strongly disturbed and of varying thickness in the western (Fig. 6D) part of the outcrop. Glauconitic clay, which usually occurs between limestone and argillite, is missing here. Black argillite can be found squeezed into the faults of the overlying limestone.

Deformations become even more severe some tens of meters to the west of the cliff, where the Ordovician and Cambrian sandstone and siltstone blocks of different sizes and orientations (including those turned upright) occur at the upper level of the cliff. The bedrock blocks are vertically intersected by a glacial till dike that seems to continue near the seashore in the blue clay that rises above sea level (several meters higher than in the eastern part of the cliff).

Half a kilometer to the southeast of the Udria cliff, between Udria and Meriküla villages, lies a flat limestone plateau that can be divided into two separate blocks (Fig. 3B). These blocks have subhorizontal bedding with little internal topography, suggesting that the carbonate rocks have not moved much (if at all) relative to the underlying Ordovician and Cambrian sandstones. The blocks, measured about 1.5 km in the NE–SW direction and 300–400 m in the NW–SE direction, are separated by inclined bedding (Fig. 3A). A narrow (60–100 m wide) anticlinal structure was detected in the radar images (Fig. 2B).

The Udria cliff suggests that argillite is the weak layer at which carbonate bedrock layers are detached from the underlying bedrock and can move over the crushed/deformed layers. A compressional deformation zone between internally weakly deformed and subhorizontal limestone blocks indicates that sometimes limestone in larger blocks is not detached from the underlying Ordovician and Cambrian sandstones, and décollement occurs at greater depth, in the blue clay formation.

Puhkova

In Puhkova village, wavy, folded, and thrusted carbonate rock blocks form 1–3 m high ridge-like features that can

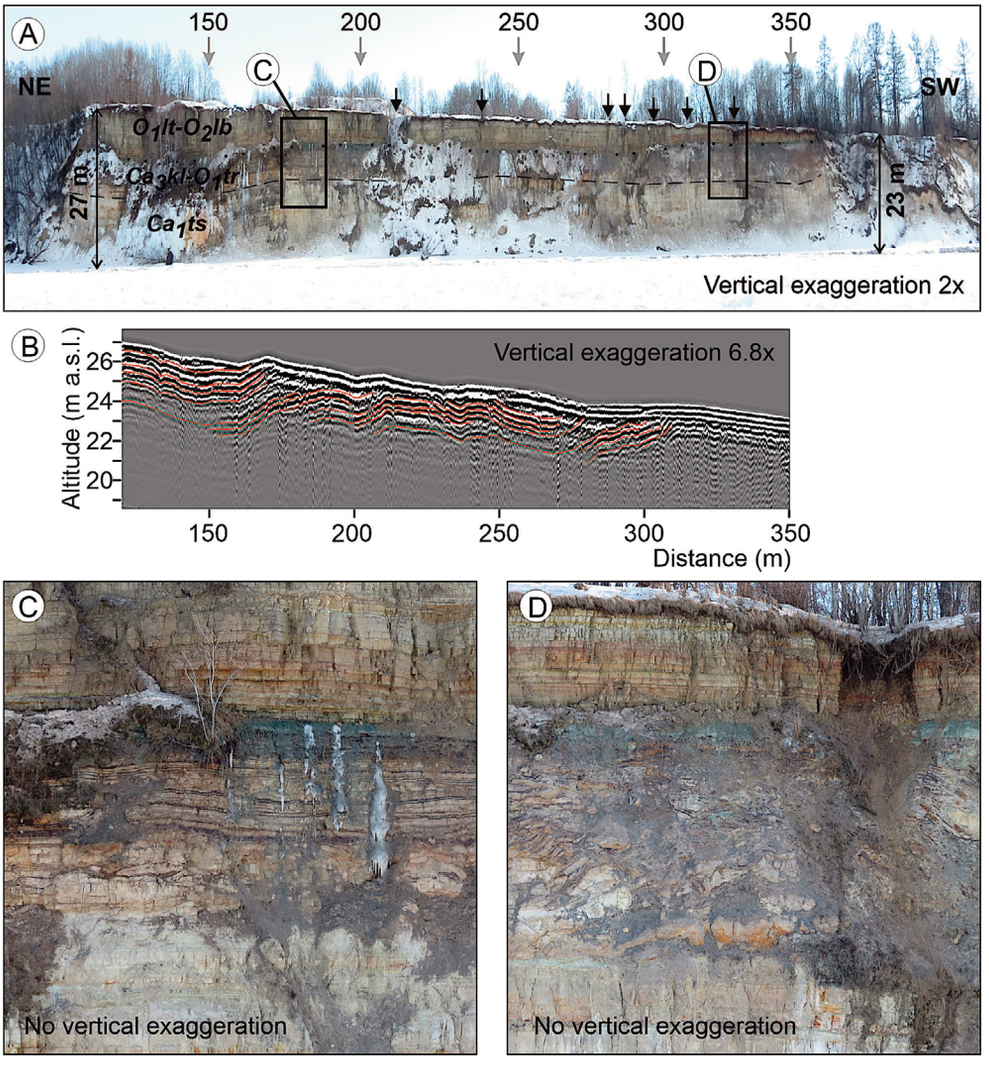

Fig. 6. A – Photo of the Udria cliff from sea ice. The dotted line marks the base of the limestone that lies on top of the clay rock-argillite layers (lower boundary is marked by a dashed line) and sandstone. Black arrows indicate faults in the carbonate rocks. B – GPR profile was recorded 20–30 m south of the cliff edge (approximate location of the profile is marked on A). Note the differences in internal disturbances in the clay rock-argillite complex under the seemingly undisturbed limestone complex in the eastern (C) and western (D) parts of the cliff.

be lineated in the DEM (Fig. 3B). In the GPR sections, the apparent dip angle of the fold limbs is less than 10°, occasionally there are folds with a true dip angle of the limbs up to 27°. However, field observations also show dips in the range of 60–90°, indicating that the steep tilting of the bedrock and the relief of the ridges do not allow the detection of all bedrock features in the GPR sections.

The ridges are located to the north of the erratic bank of Sõmerkallas. Figure 2D shows a GPR profile where at 0–100 m sandstones and limestones of the large block of Sõmerkallas are tilted, but otherwise apparently not deformed. The northern part of the profile shows folded carbonate rocks in the core of the ridge. In the case of some ridges, folds with steeply tilted limbs and thrusted blocks cannot be differentiated. As a general observation, deformations of types II and III predominate close to the Sõmerkallas block whereas types I and II prevail further north.

Deformations at margins and outside the VDZ

The south(east)ern border of the VDZ (Fig. 1) limits most of the deformations. Further southwards the carbonate bedrock may have tilted somewhat differently from the regional dip, but wavy bedding is lacking. The Sinimäed Hills and the Laagna rise are large positive landforms; in the rest of the VDZ margin, the carbonate rocks rise

towards the VDZ in a relatively narrow zone associated with no significant topography.

To the east of the VDZ, the Baltic Klint turns southeast, having two linear segments of the same orientation. Carbonate bedrock deformations occasionally occur near the Klint line. There are a few locations where carbonate bedrock blocks extend northeast from the Klint line. Near Tõrvajõe, one hill is clearly composed of a pile of limestone and sandstone blocks (Fig. 4A). The other block seems undisturbed and not rotated (Plado et al. 2016). The Pähklimäed Hills are composed of 4–5 closely spaced blocks of carbonate rocks that have different tilt angles and directions (Fig. 4B), being erratic.

Several GPR profiles were drawn for archaeological purposes within the Narva Old Town (Plado and Davydov 2019; Fig. 4B). Among archaeological features, the GPR data revealed reflections from sedimentary layers, presumably limestones and marlstones of the Middle Ordovician age (Suuroja et al. 2009a). The strike of the bedding was found to be directed SSW–NNE with a dip towards ESE. The maximum dip angle (3.2°) toward 260° was measured on a west-east running profile (Fig. 5B). Thus, it seems that Narva Old Town is built on the eastern side of a voluminous (1.0 × 1.2 km in a plan view) glacially drifted block.

Usability of GPR

The performance of GPR in mapping the stratigraphy of soil and rock and the high-resolution results obtained by variable-scaled GPR studies of limestone and crystalline rocks are well documented in the literature (e.g., Liner and Liner 1995; Sigurdsson and Overgaard 1998; Pipan et al. 2000; Zajc et al. 2015; Elkarmoty et al. 2018). Our study shows that the Quaternary cover and the underlying bedrock – either limestones, dolostones, or sandstones – are well discriminated under the thin Quaternary cover. Occasionally, bedrock formations can be distinguished in the radar images, primarily due to differences in clay content. For example, the lowermost part of the carbonate rock sequence within the VDZ, the glauconitic limestones of the Toila Formation, is rich in clay, thus attenuating electromagnetic signals well.

Our study shows that bedrock structures can be observed under a few meters of marine and coastal sand and gravel. In contrast, till, which is rich in blue clay, and clayey bedrock units (argillite and blue clay) attenuate the GPR signal rapidly and do not allow the identification of bedrock structures. Meadows with long grass and roads with clayey filling seem to block the GPR signal effectively. Thus, there are several factors that hinder visibility in radar images, and it is not easy to understand what the specific cause is.

The reflection pattern of limestone is strongly affected by the intensity of deformation. A flat limestone plateau is characterized by long continuous horizontal or slightly undulating bedding. However, ruptured and fractured limestone, and deformed sandstone may provide similar non-continuous and fragmentary GPR images, which are therefore undistinguishable by the radar method alone. Due to the similarity between the ruptured limestone and sandstone in the GPR images, the thick (clayey) Quaternary cover, and the unfavorable vegetation, GPR alone is not sufficient to outline the deformed limestone blocks. To delineate the blocks, a further combination of geophysical (e.g., seismic, electric, electromagnetic), (bio)geological, and topographical (DEM) sources is needed.

CONCLUSIONS

Previously, ground-penetrating radar has been used for describing glaciotectonic deformations in soft Quaternary sediments, as well as pre-Quaternary tectonic features in consolidated bedrock. For the first time GPR was applied to identify, delineate, and describe Quaternary-aged deformations within the layered Ordovician bedrock. High-resolution radar images enable the detection of bedrock tilting and other structural elements that are presumably characteristic of the deeper part of the section. The deformations in carbonate rocks range from weak (wavy bedding, i.e., low amplitude folds, tilting that exceeds regional values) to strong (folds with steep limbs, thrusting). Most of the deformations were identified within the Vaivara Deformation Zone, but occasionally shifted and tilted blocks occur eastward from the VDZ. The distribution and nature of deformations hint at the glaciotectonic origin whereas the intensity of deformations is linked to the range of horizontal shortening.

Acknowledgements. We thank the last and previous glaciers for deforming the area and providing us with a beautiful natural laboratory for testing the geophysical instruments and methods. We are grateful to Kalle-Mart Suuroja and Kuldev Ploom for fruitful discussions on the geology of the study area. Kristjan Rooni is acknowledged for supporting activities during the fieldwork. The study was partly financed by the Estonian Science Foundation grant No. 7860. The authors are grateful to Hannes Tõnisson and an anonymous reviewer for their valuable comments. The publication costs of this article were covered by the Estonian Academy of Sciences.

REFERENCES

Aber, J. S. and Ber, A. 2007. *Glaciotectonism.* Developments in Quaternary Science Series, Vol. 6. Elsevier, Amsterdam.

Bakker, M. A. J. and van der Meer, J. J. M. 2003. Structure of a Pleistocene push moraine revealed by GPR: the eastern

Veluwe Ridge, The Netherlands. *Geological Society, London, Special Publications*, **211**, 143–151.

Brandes, C. and Le Heron, D. P. 2010. The glaciotectonic deformation of Quaternary sediments by fault-propagation folding. *Proceedings of the Geologists' Association*, **121**, 270–280.

Busby, J. P. and Merritt, J. W. 1999. Quaternary deformation mapping with ground penetrating radar. *Journal of Applied Geophysics*, **41**(1), 75–91.

Ehlers, J. and Gibbard, P. L. 2003. Extent and chronology of glaciations. *Quaternary Science Reviews*, **22**, 1561–1568.

Elkarmoty, M., Tinti, F., Kasmaeeyazdi, S., Bonduà, S. and Bruno, R. 2018. 3D modeling of discontinuities using GPR in a commercial size ornamental limestone block. *Construction and Building Materials*, **166**, 81–86.

Fitzsimons, S. and Howarth, J. 2020. Development of push moraines in deeply frozen sediment adjacent to a cold-based glacier in the McMurdo Dry Valleys, Antarctica. *Earth Surface Processes and Landforms*, **45**(3), 622–637.

Ingólfsson, Ó., Benediktsson, Í. Ö., Schomacker, A., Kjær, K. H., Brynjólfsson, S., Jónsson, S. A. et al. 2016. Glacial geological studies of surge-type glaciers in Iceland – Research status and future challenges. *Earth-Science Reviews*, **152**, 37–69.

Jõeleht, A. and Plado, J. 2010. Architecture of the northeastern rim of the Kärdla impact crater, Estonia, based on ground-penetrating radar studies. In *Large Meteorite Impacts and Planetary Evolution IV* (Gibson, R. L. and Reimold, W. U., eds). *The Geological Society of America Special Paper*, **465**, 133–140.

Karukäpp, R. and Raukas, A. 1997. Deglaciation history. In *Geology and Mineral Resources of Estonia* (Raukas, A. and Teedumäe, A., eds). Estonian Academy Publishers, Tallinn, 263–267.

Liner, C. L. and Liner, J. L. 1995. Ground-penetrating radar: a near-face experience from Washington County, Arkansas. *The Leading Edge*, **14**(1), 17–21.

Lobanov, J. N. 1976. О природе дислокаций Дудергофских высот в окрестностях Ленинграда (The character of deformation in Dudergof Heights near Leningrad). *Геотектоника*, **6**, 89–98 (in Russian).

Meidla, T. 2014. Estonia – a Palaeozoic country. In *Proceedings of the 4th Annual Meeting of IGCP 591, Estonia, 10–19 June 2014. Abstracts and Field Guide* (Bauert, H., Hints, O., Meidla, T. and Männik, P., eds.). University of Tartu, Tartu, 111–113.

Møller, I. and Jakobsen, P. R. 2002. Sandy till characterized by ground-penetrating radar. In *Proceedings of the Ninth International Conference on Ground Penetrating Radar, Santa Barbara, CA, USA, 29 April–2 May 2002* (Koppenjan, S. and Lee, H., eds.). SPIE, **4758**, 308–312.

Mustasaar, M., Plado, J. and Jõeleht, A. 2011. Determination of electromagnetic wave velocity in horizontally layered sedimentary target: a ground-penetrating radar study from Silurian limestones, Estonia. *Acta Geophysica*, **60**(2), 357–370.

Overgaard, T. and Jakobsen, P. R. 2001. Mapping of glaciotectonic deformation in an ice marginal environment with ground penetrating radar. *Journal of Applied Geophysics*, **47**(3–4), 191–197.

Pasanen, A. 2009. Radar stratigraphy of the glaciotectonically deformed deposits in the Isoniemi area, Haukipudas, Finland. *Bulletin of the Geological Society of Finland*, **81**(1), 39–51.

Pipan, M., Baradello, L., Forte, E. and Prizzon, A. 2000. GPR study of bedding planes, fractures, and cavities in limestone. In *Proceedings of the Eighth International Conference on Ground Penetrating Radar* (Noon, D. A., Stickley, G. F. and Longstaff, D., eds). *SPIE,* **4084,** 682–687.

Plado, J. and Davydov, I. 2019. Ground-penetrating radar studies in Narva at Tuleviku 9 and neighboring cadastral units. Study Report. Department of Geology, University of Tartu (in Estonian).

Plado, J., Preeden, U., Jõeleht, A., Pesonen, L. J. and Mertanen, S. 2016. Palaeomagnetism of Middle Ordovician carbonate sequence, Vaivara Sinimäed area, northeast Estonia, Baltica. *Acta Geophysica*, **64**(5), 1391–1411.

Puura, V. and Vaher, R. 1997. Deep structure. In *Geology and Mineral Resources of Estonia* (Raukas, A. and Teedumäe, A., eds). Estonian Academy Publishers, Tallinn, 163.

Rattas, M. and Kalm, V. 2004. Glaciotectonic deformation pattern in Estonia. *Geological Quarterly*, **48**(1), 15–22.

Raukas, A. 1995. Estonia – a land of big boulders and rafts. *Questiones Geographicae, Special issue,* **4**, 247–253.

Shihab, S., Al-Nuaimy, W. and Eriksen, A. 2004. Radius estimation for subsurface cylindrical objects detected by ground penetrating radar. In *Proceedings of the Tenth International Conference on Ground Penetrating Radar*, *Delft, The Netherlands, 21–24 June 2004* (Slob, E. C., Yarovoy, A. G. and Rhebergen, J. B., eds). IEEE, 319–322.

Sibul, I., Plado, J. and Jõeleht, A. 2017. Ground-penetrating radar and electrical resistivity tomography for mapping bedrock topography and fracture zones: a case study in Viru-Nigula, NE Estonia. *Estonian Journal of Earth Sciences*, **66**(3), 142–151.

Sigurdsson, T. and Overgaard, T. 1998. Application of GPR for 3-D visualization of geological and structural variation in a limestone formation. *Journal of Applied Geophysics*, **40**(1–3), 29–36.

Suuroja, K. and Ploom, K. 2016. Vaivara Sinimägede ja dislokatsioonide vööndi tekkest (On the formation of Vaivara Sinimäed and dislocation zone). *Bulletin of the Geological Survey of Estonia*, **12**, 37–56 (in Estonian).

Suuroja, K., Mardim, T., Ploom, K., All, T., Otsmaa, M. and Kõiv, M. 2009a. *Eesti geoloogilise baaskaardi Narva (6534) leht. Seletuskiri* (*The explanatory note to the geological maps of Narva (6534) sheet*). Geological Survey of Estonia, Tallinn (in Estonian).

Suuroja, K., Mardim, T., Ploom, K., All, T., Kõiv, M. and Otsmaa, M. 2009b. *Eesti geoloogilise baaskaardi Sillamäe (6533) leht. Seletuskiri* (*The explanatory note to the geological maps of Sillamäe (6533) sheet*). Geological Survey of Estonia, Tallinn (in Estonian).

Tuuling, I. and Flodén, T. 2016. The Baltic Klint beneath the central Baltic Sea and its comparison with the North Estonian Klint. *Geomorphology*, **263**, 1–18.

Vaher, R., Miidel, A. and Raukas, A. 2013. Structure and origin of the Vaivara Sinimäed hill range, Northeast Estonia. *Estonian Journal of Earth Sciences*, **62**(3), 160–170.

Volin, A. 1974. Диапировые структуры окрестностей Ленинграда (Diapiric structures around Leningrad). *Природная обстановка и фауна прошлого*, **8**, 142–150 (in Russian).

Zajc, M., Celarc, B. and Gosar, A. 2015. Structural–geological and karst feature investigations of the limestone–flysch thrust-fault contact using low-frequency ground penetrating radar (Adria–Dinarides thrust zone, SW Slovenia). *Environmental Earth Sciences*, **73**, 8237–8249.

Kirde-Eesti aluspõhja deformatsioonid georadari läbilõigetel

Argo Jõeleht, Ivo Sibul, Mario Mustasaar ja Jüri Plado

Georadariga uuriti Kirde-Eestis asuvat Vaivara deformatsioonide vööndit. Kui tüüpilist Põhja-Eesti karbonaatkivimite platood iseloomustab georadari läbilõigetel subhorisontaalne ja pidev peegeldusmuster, siis deformatsioonide vöönd sisaldab häiritud ja kallutatud peegeldusi. Artiklis on liigitatud georadari läbilõigetel nähtavad peegeldused vastavalt deformatsioonide intensiivsustele ning on kirjeldatud deformatsioonide pindalalist jaotust. Lisaks Vaivara deformatsioonide vööndile on kallutatud aluspõhja plokke kirjeldatud Tõrvajõe külas, Pähklimägedes ning Narva linnas. Deformatsioonide levik ja olemus viitab glatsiotektoonilisele päritolule. Uuring kinnitab, et georadar on sobiv vahend aluspõhja struktuuride avastamiseks ja iseloomustamiseks. Erineva koostisega aluspõhjaliste plokkide kontuurimiseks on vaja teostada täiendavaid geoloogilisi ja geofüüsikalisi uuringuid.